Appl Phys B (2010) 100: 515–520
DOI 10.1007/s00340-010-4102-y

Applied Physics B
Lasers and Optics

Filament-induced laser machining (FILM)

D. Kiselev · L. Woeste · J.-P. Wolf

Received: 25 May 2010 / Published online: 30 June 2010

Abstract Laser filamentation provides high intensity plasma strings of micrometric diameters and lengths of tens of centimeters. We demonstrate that these filaments can be used for remotely drilling and cutting metals and biological materials such as flesh and bones. Since no tight focusing is needed, complex 3D shapes can be machined without any adjustment of the laser while processing.

1 Introduction

Above a critical power (3 GW in air), ultrashort laser pulses undergo filamentation while propagating through transparent media [1–4]. Filamentation is a self-sustained non-linear propagation mode that produces filaments of light of micrometric diameters over tens of centimeters length. The process stems from a dynamical balance between non-linear Kerr indices of alternating signs and defocussing by the self-generated plasma. Attractive properties of filaments (remote delivery of high intensities, supercontinuum generation, and electric conductivity) have recently induced a wealth of atmospheric applications such as pollution monitoring [2, 5, 6], lightning control [7] and water vapor condensation [8]. The interaction of laser filaments with solid targets has been mainly exploited for generating structures such as waveguides in glass [9, 10] or analysis purposes, such as remote LIBS (Laser-Induced Breakdown Spectroscopy) analysis of metals and chemicals [11–14] and bacteria [15–17]. Their unique self-guiding property indeed opened new perspectives for LIBS-analysis of targets at distances widely extending the Rayleigh lengths, i.e. typically hundred meters [18].

Here, we show the capabilities of filaments for laser machining, and call it FILM, for "Filament-Induced Laser Machining". More precisely, we demonstrate the remote drilling of micrometric holes without focusing, the cutting of complex shaped 3D objects in various metals and biomaterials, and the use of background-free LIBS spectra for analyzing the samples.

2 Experimental

The experimental set-up is shown in Fig. 1. A chirped-pulse-amplified (CPA) Ti:Sapphire laser system emits 1.5 mJ, 80 fs pulses at 800 nm and 1 kHz repetition rate. The pulse duration can be modified from 80 fs to 1 ps by impinging a chirp within the laser compressor. The beam of 15 mm diameter is softly focused on the sample using a long focal length lens ($f = 1$ m). The samples, which consist of metal objects and biological materials, are scanned across the filaments using a 2D micro positioning stage. Previous experiments showed [1–4] that the intensity inside the filaments (~ 100 μm diameter) was clamped to a typical value in air of 10^{13} W/cm^2, associated with a self-generated plasma density of 10^{15}–10^{16} cm^{-3}. Notice also that the initial pulse duration is strongly affected by the filamentation process, leading for instance to self-shortening and pulse splitting [19, 20]. If the laser power largely exceeds some critical

D. Kiselev · J.-P. Wolf (✉)
GAP-Biophotonics, Univertsité de Genève, 20 Ecole de Médecine, 1211 Geneva 4, Switzerland
e-mail: jean-pierre.wolf@unige.ch

D. Kiselev
e-mail: denis.kiselev@unige.ch

L. Woeste
Institut für Experimentalphysik, Freie Universität Berlin, Arnimallee 14, 14195 Berlin, Germany
e-mail: ludger.woeste@physik.fu-berlin.de

Fig. 1 Experimental set-up

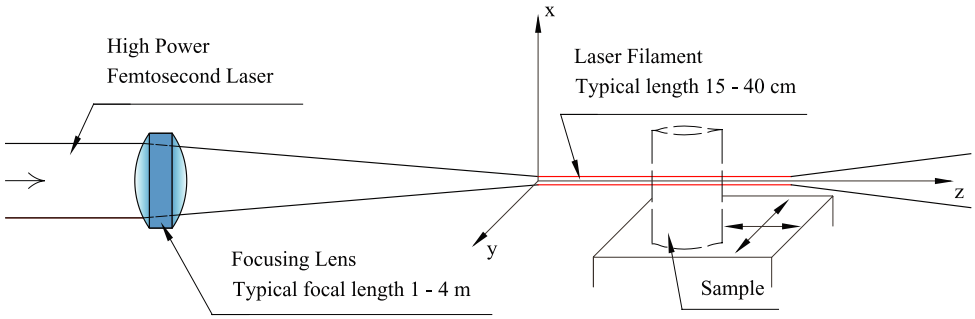

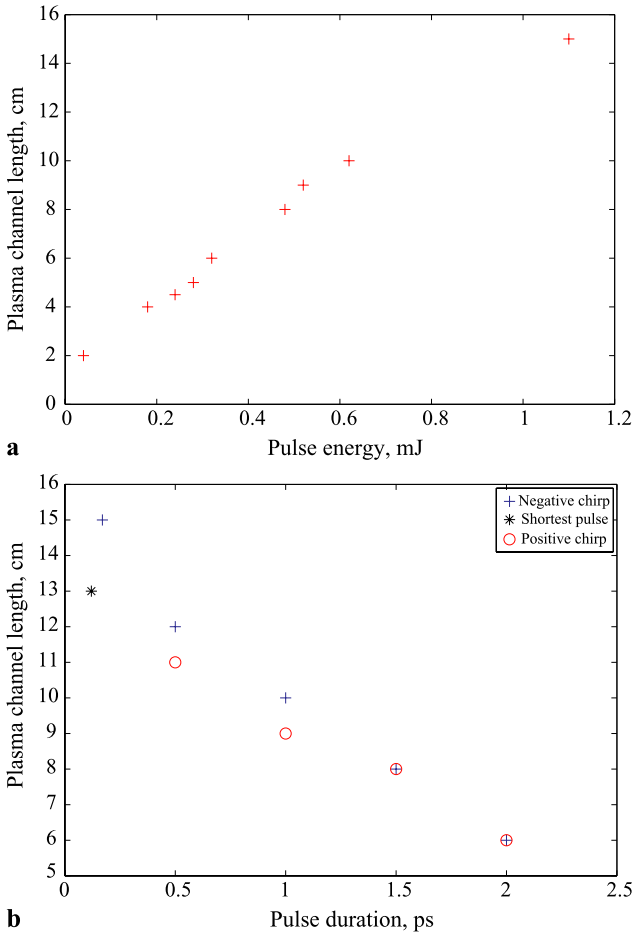

Fig. 2 Filament length as a function of laser parameters: (**a**) energy, (**b**) pulse duration (chirped pulse)

powers P_c (3 GW in air), the beam usually breaks up in several filaments, bearing each 1–5 P_c. In our case, the maximal peak power of $P = 12$ GW would support the creation of some filaments. However, initial focusing of the beam often leads to geometric merging of multiple filaments in a single plasma channel.

Figure 1a displays the filament length (measured using laser impacts on a solid target) as a function of the initial laser energy and with pulse duration 80 fs. The filament length reaches 15 cm for an incoming energy of 1.1 mJ, i.e. widely exceeding the linear Rayleigh limit for this laser beam ($2Z_R = 10$ mm). Reducing the energy yields an almost linear decrease of the filament length down to a few cm for 0.2 mJ, i.e. roughly $1P_c$. It is important to notice that both filament onset and length are very sensitive to the spatial beam profile and especially to astigmatism and spatial chirp. A further control of the filament length is provided by the initial pulse duration and chirp (Fig. 2b). These measurements must, however, be taken cautiously as filamentation strongly modifies the temporal profile of the pulse while propagating. It is, for instance, well known that pulse shortening and steepening occurs within the filaments (down to some femtoseconds [20]) as well as pulse splitting [19]. Nevertheless the filament length clearly decreases with the initial pulse duration (except for the longest filament where a small initial negative chirp is needed, see below), according to the decreasing P/P_c ratio. A slight asymmetry is observed between negative and positive chirps in favor of the negative one. A simple explanation could be a first order compensation of group velocity dispersion (GVD) in the focusing lens. Considering the short distances involved, GVD in air can be fully neglected.

3 Results

3.1 Remote and focus-less drilling of metal samples using FILM

Since filaments provide a long "extended focus" over several centimeters, holes are drilled in targets all along this large distance. As shown in Fig. 3, holes of typically 50–100 μm in diameter (Fig. 4) have been remotely drilled in foils (0.5 mm thickness) of aluminum, brass and stainless steel. Within the filament because of intensity clamping, the drilling time is rather constant in the 10-s range, while it steeply rises to several minutes just at the onset and at the end of it. No drilling was observed outside the filament region. For aluminum and brass, drilling was successful within a distance interval exceeding 13 cm (corresponding to the

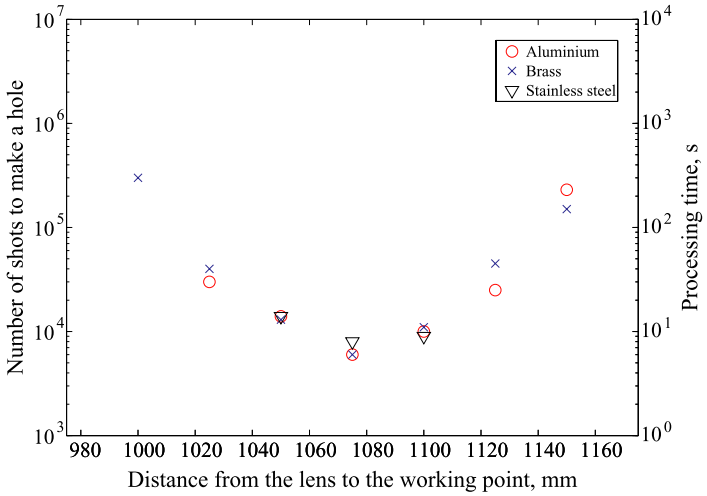

Fig. 3 FILM based drilling in aluminum, brass, and stainless steel

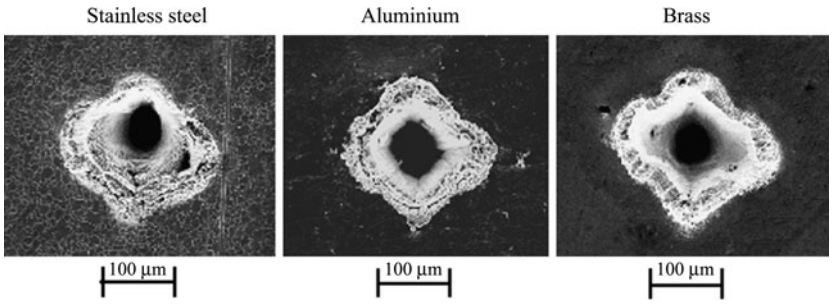

Fig. 4 SEM images of 50 µm holes drilled in stainless steel (**a**), aluminum (**b**) and brass (**c**)

short drilling times). Stainless steel was obviously more difficult to process as it could only be machined in the region where the filament was the strongest over a distance of 5 cm. Figure 4 compares the drilling quality and hole size for the 3 metal foils and 10 s processing time. The diameters are similar, about 50 µm, while the asymmetric shape of the surrounding crater suggests some astigmatism of the incoming laser beam. Depending on the processing time (i.e. the number of laser shots) the hole size could be modified from typically 10–200 µm. Compared to the standard tightly focused configuration [21, 22], filaments create holes of comparable quality but do not reach the state-of-the-art standards [23]. Material re-deposition around the crater is clearly visible, and would need post-processing measures to clean it. Optimizing the repetition rate or processing under some gas flow could also be useful to reduce the problem in the future [21, 24, 25]. The ablation rate is typically 0.05–0.1 µm/pulse, similar to the rate observed for femtosecond lasers in the focused configuration and comparable fluences (some J/cm^2) [25].

These results clearly demonstrate the remote and focusless drilling capability of filaments. The position of the sample can be freely chosen within the filament length, and can have any orientation with respect to the laser axis. A complete parametric investigation should be obviously realized for optimizing the laser parameters (soft focusing length, energy, duration, repetition rate, etc.) for each application, but this is beyond the scope of the present paper.

An important remark for FILM is the role of the surrounding "photon bath", which constitutes a serious limiting factor for drilling holes with high aspect ratios. As described in the introduction, filamentation stems from a dynamic balance between self-focusing and defocussing by the self-generated plasma. This implies that the light surrounding the filament plays an important role as an energy reservoir, or photon bath where energy is permanently exchanged with the filament. Therefore, if the photon bath is cut by a diaphragm, filamentation stops [26]. In opposite, if only the filament is cut by an obstacle, the surrounding photon bath regenerates a filament after this obstacle [27]. In the case of drilling hole, the photon bath is mainly cut by the material, which prevents further propagation and thus drilling of the material. In our case, the maximal material thickness that could be drilled with FILM was 2 mm, i.e. a maximal aspect ratio of 1:20. This clear limitation, as compared to state-of-the-art femtosecond laser machining [28] has to be kept in mind while envisaging further applications: if the material is not transparent FILM can only machine foils (otherwise the bath can propagate through the material, which allows further filament propagation). Foils can form complex 3D objects as shown below, but drilling trough thick metallic material is out of reach for FILM.

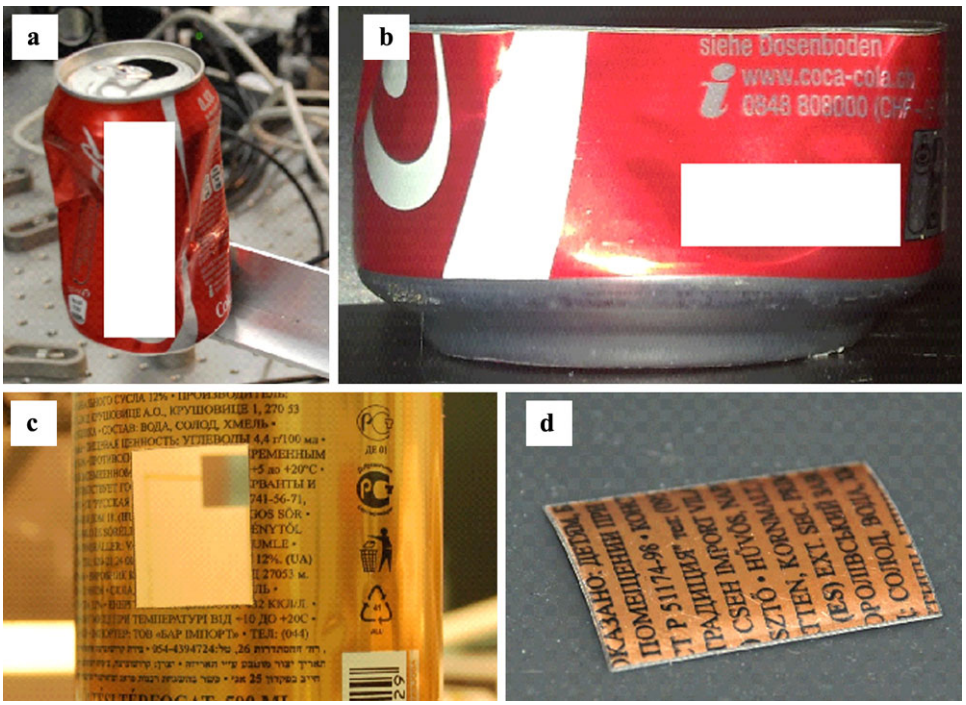

Fig. 5 Filament saw applied to the focus-less cutting of an aluminum can (**a**) + (**b**); throughout horizontal cut; (**c**) + (**d**): Cut of a 4 × 2 cm window on the curved surface of a can

3.2 Remote and focus-less cutting of metal samples

Thank to its extended plasma string geometry, filaments act as a laser saw. In order to demonstrate this capability, we first saw throughout an extended 3D metallic object, namely a deformed aluminum can. The can diameter (5 cm) and wall thickness (0.2 mm) were typical for this kind of sample. As can be seen in Figs. 5(a)–5(b) the can was cut perfectly horizontally (i.e. parallel to the translation stage motion) regardless of its complex shape. Using standard focusing techniques, this would have required an extensive focus adaptation while cutting and a rotation over 360° of the object, provided the object was void and reasonably regular. In other cases (object containing a structure or object with sharp concave curvatures) such a cut would be impossible using focused laser techniques. As an alternative, a rectangular window of 4 × 2 cm was cut in a similar cylindrical object (Figs. 5(c)–5(d)), showing the capability of sawing rectangular shapes on a curved surface. The quality of machining and surface aspect after processing are excellent, as shown in Fig. 5c, with excellent regularity and no damage (burns, thermal deformation) of the edges. Obviously, a symmetric window could have been cut on the opposite face simultaneously if desired, without rotating the object.

An attractive feature of FILM is that it can be performed remotely, i.e. in hostile environments and/or through other transparent media than air. In particular it was demonstrated that filaments survive adverse conditions like turbulence [29, 30] or turbidity [30, 31]. The process is also known to occur in bulk transparent media such as glass or water; the properties of the generated filaments are, however, modified by the medium so that machining experiments should be investigated specifically in these media.

The cutting time was, however, in this extended filament geometry, significant: 10 min for the window of Figs. 5(c)–5(d). The reason for this is mainly a compromise between filament length and plasma density/peak intensity. Again, depending on the initial conditions (energy, pulse duration, beam diameter, soft focusing lens focal length), the filament onset and length can be modulated, however on the price of the peak local intensity. Therefore, depending on the application it will be more appropriate to use longer filaments/longer processing time or shorter filaments/shorter processing time.

3.3 Simultaneous LIBS analysis of the samples

Using ultrashort laser pulses provides the attractive advantage of generating low thermal background, and therefore high contrast on the plasma lines. The reason is that plasma heating by inverse Bremsstrahlung and further cascade ionization has no time to take place at these time scales. Accordingly plasma lines emitted by the air molecules around the sample are almost avoided. While FILM processing, clean plasma fluorescence is therefore emitted by the sample only, as shown in Fig. 6, although no temporal gating of the blackbody background was used. The characteristic plasma lines for aluminum, copper and stainless steel are clearly identified, allowing on-line analysis of the composition of complex object and even feed back optimization [32]

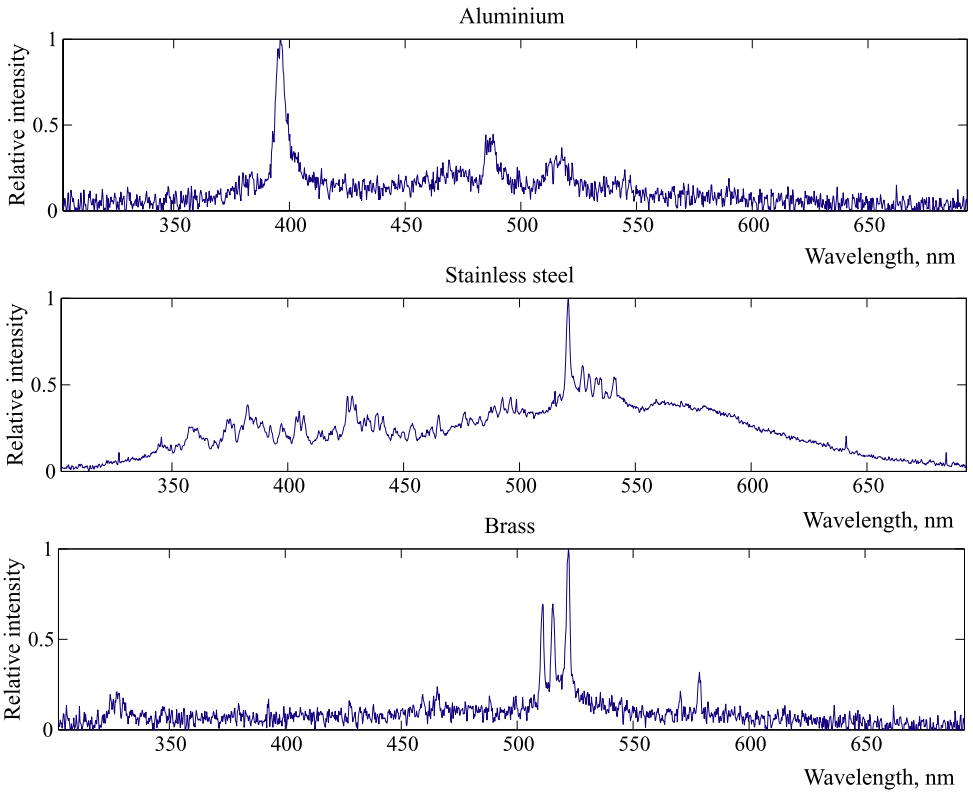

Fig. 6 LIBS analysis of the samples while processing with laser filaments

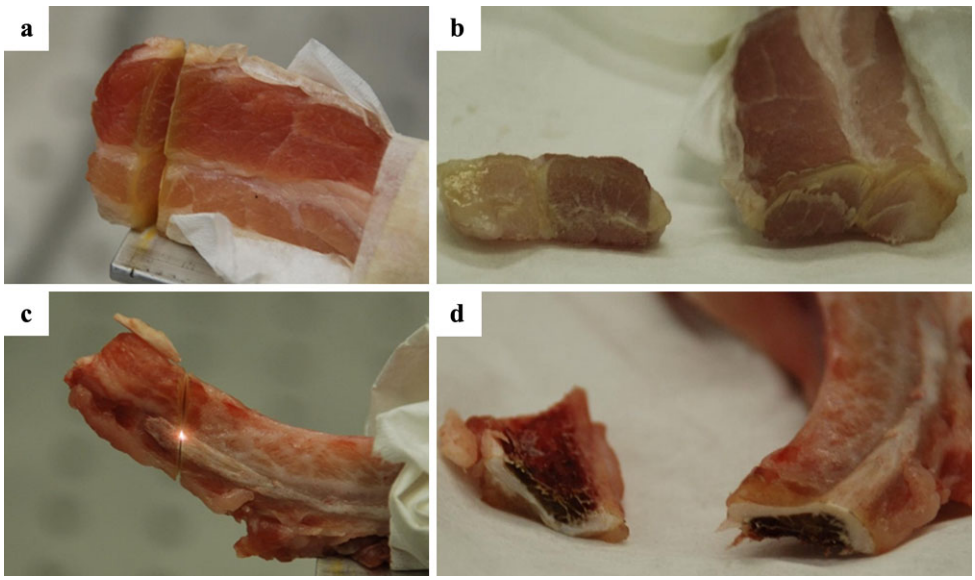

Fig. 7 FILM sawing of biological samples: flesh ((**a**) + (**b**) and bones ((**c**) + (**d**))

while processing. Traditional temporal gating of the ICCD camera of the spectrometer can obviously be applied to further improve the contrast and identify traces elements within the samples.

3.4 FILM sawing of biological material

Another application of filament-induced laser machining could arise in the biomedical sector. In order to assess the capabilities of FILM for surgery, we investigated remote sawing of soft biomaterial such as flesh and hard materials such as bones (Fig. 7). In both cases, FILM successfully fulfilled the task, and allowed a very clean cut, without burning signs or overheating of the borders. It is however important to notice that the processing time was again excessively long (typically 10 min) so that a significant scaling in laser power would be required for this kind of surgery. Appropriate applications might therefore be microsurgery where

smaller cuts are needed with high precision and low collateral damages.

Acknowledgements We wish to express our gratitude to the *Schweizerischer Nationalfonds*, the *Deutsche Forschungsgemeinschaft (Sfb 450)* and the *Schmidheiny Foundation* for supporting this binational scientific cooperation project.

References

1. L. Bergé, S. Skupin, R. Nuter, J. Kasparian, J.-P. Wolf, Rep. Prog. Phys. **70**, 1633 (2007)
2. J. Kasparian, J.-P. Wolf, Opt. Express **16**, 466 (2008)
3. S.L. Chin, S.A. Hosseini, W. Liu, Q. Luo, F. Theberge, N. Akozbek, A. Becker, V.P. Kandidov, O.G. Kosareva, H. Schroeder, Can. J. Phys. **83**, 863 (2005)
4. A. Couairon, A. Mysyrowicz, Phys. Rep. **441**, 47 (2007)
5. J. Kasparian, M. Rodriguez, G. Méjean, J. Yu, E. Salmon, H. Wille, R. Bourayou, S. Frey, Y.-B. André, A. Mysyrowicz, R. Sauerbrey, J.-P. Wolf, L. Wöste, Science **301**, 61 (2003)
6. G. Méjean, J. Kasparian, J. Yu, S. Frey, E. Salmon, J.-P. Wolf, Appl. Phys. B **78**, 535 (2004)
7. J. Kasparian, R. Ackermann, Y.B. Andre, B. Prade, G. Mechain, G. Méjean, P. Rohwetter, E. Salmon, V. Schlie, J. Yu, A. Mysyrowicz, R. Sauerbrey, L. Wöste, J.P. Wolf, Opt. Express **16**(8), 5757 (2008)
8. P. Rohwetter, J. Kasparian, K. Stelmaszczyk, Z. Hao, S. Henin, N. Lascoux, W.M. Nakaema, Y. Petit, M. Queißer, R. Salame, E. Salmon, L. Woste, J.-P. Wolf, Nat. Photon. (2010). DOI:10.1038/nphoton.2010.115
9. D.G. Papazoglou, I. Zergioti, S. Tzortzakis, Opt. Lett. **32**, 2055 (2007)
10. W. Watanabe, Y. Note, K. Itoh, Opt. Lett. **30**, 2888 (2005)
11. Ph. Rohwetter, K. Stelmaszczyk, L. Wöste, R. Ackermann, G. Méjean, E. Salmon, J. Kasparian, J. Yu, J.P. Wolf, Spectrochim. Acta B **60**, 1025 (2005)
12. H.L. Xu, J. Bernhardt, P. Mathieu, G. Roy, S.L. Chin, J. Appl. Phys. **101**, 033124 (2007)
13. J.-F. Daigle, G. Méjean, W. Liu, F. Théberge, H.L. Xu, Y. Kamali, J. Bernhardt, A. Azarm, Q. Sun, P. Mathieu, G. Roy, J.-R. Simard, S.L. Chin, Appl. Phys. B **87**, 749 (2007)
14. J.-F. Daigle, P. Mathieu, G. Roy, J.-R. Simard, S.L. Chin, Opt. Commun. **278**, 147 (2007)
15. M. Baudelet, J. Yu, M. Bossu, J. Jovelet, J.-P. Wolf, T. Amodeo, E. Fréjafon, P. Laloi, Appl. Phys. Lett. **89**, 163903 (2006)
16. M. Baudelet, L. Guyon, J. Yu, J.P. Wolf, T. Amodeo, E. Fréjafon, P. Laloi, Appl. Phys. Lett. **88**, 053901 (2006)
17. H.L. Xu, G. Méjean, W. Liu, Y. Kamali, J.-F. Daigle, A. Azarm, P.T. Simard, P. Mathieu, G. Roy, J.-R. Simard, S.L. Chin, Appl. Phys. B **87**, 151 (2007)
18. K. Stelmaszczyk, Ph. Rohwetter, G. Méjean, J. Yu, E. Salmon, J. Kasparian, R. Ackermann, J.P. Wolf, L. Woeste, Appl. Phys. Lett. **85**(18), 3977 (2004)
19. D. Faccio, M.A. Porras, A. Dubietis, F. Bragheri, A. Couairon, P. Di Trapani, Phys. Rev. Lett. **96**, 193901 (2006)
20. S. Skupin, G. Stibenz, L. Berge, F. Lederer, T. Sokollik, M. Schnurer, N. Zhavoronkov, G. Steinmeyer, Phys. Rev. E **74**, 056604 (2006)
21. C.Y. Chien, M.C. Gupta, Appl. Phys. A **81**, 1257 (2005)
22. S. Juodkazis, H. Okuno, N. Kujime, S. Matsuo, H. Misawa, Appl. Phys. A **79**, 1555 (2004)
23. G. Kamlage, T. Bauer, A. Ostendorf, B.N. Chichkov, Appl. Phys. A **77**, 307 (2003)
24. K. Chen, Y.L. Yao, V. Modi, J. Manuf. Sci. Eng. **122**, 429 (2000)
25. C.S. Nielsen, P. Balling, J. Appl. Phys. **99**, 093101 (2006)
26. W. Liu, F. Theberge, E. Arevalo, J.F. Gravel, A. Becker, S.L. Chin, Opt. Lett. **30**, 2602 (2005)
27. F. Courvoisier, V. Boutou, J. Kasparian, E. Salmon, G. Méjean, J. Yu, J.P. Wolf, Appl. Phys. Lett. **83**(2), 213 (2003)
28. M.K. Bhuyan, F. Courvoisier, P.A. Lacourt, M. Jacquot, L. Furfaro, M.J. Withford, J.M. Dudley, Opt. Express **18**(2), 566 (2010)
29. G. Méjean, R. Ackermann, J. Kasparian, E. Salmon, J. Yu, J.-P. Wolf, Opt. Lett. **31**(1), 86 (2006)
30. G. Mechain, G. Méjean, R. Ackermann, P. Rohwetter, Y.B. Andre, J. Kasparian, B. Prade, K. Stelmasczyk, E. Salmon, J. Yu, W. Winn, V. Schlie, A. Mysyrowicz, R. Sauerbrey, L. Wöste, J.-P. Wolf, Appl. Phys. B **80**, 785 (2005)
31. G. Méjean, J. Kasparian, E. Salmon, J. Yu, S. Frey, J.P. Wolf, S. Skupin, A. Vincotte, R. Nuter, S. Champeaux, L. Bergé, Phys. Rev. E **72**, 026611 (2005)
32. R. Ackermann, E. Salmon, N. Lascoux, J. Kasparian, P. Rohwetter, K. Stelmasczyk, S. Li, A. Lindinger, L. Wöste, P. Béjot, L. Bonacina, J.-P. Wolf, Appl. Phys. Lett. **89**, 171117 (2006)